Journal of Hazardous Materials 452 (2023) 131224

Contents lists available at ScienceDirect

Journal of Hazardous Materials

journal homepage: www.elsevier.com/locate/jhazmat

Research Paper

Non-targeted analysis for the screening and semi-quantitative estimates of per-and polyfluoroalkyl substances in water samples from South Florida environments

Xuerong Li [a,b], Danni Cui [b], Brian Ng [a,b], Olutobi Daniel Ogunbiyi [a,b], Maria Guerra de Navarro [a,b], Piero Gardinali [a,b], Natalia Quinete [a,b,*]

[a] Department of Chemistry and Biochemistry, Florida International University, 11200 SW 8th Street, Modesto A. Maidique Campus, Miami, FL 33199, USA
[b] Institute of Environment, Florida International University, 11200 SW 8th Street, Modesto A. Maidique Campus, Miami, FL 33199, USA

HIGHLIGHTS

- A method based on online-solid phase extraction LC-HRMS was developed for NTA of PFAS.
- PFAS species were tentatively identified using Compound Discoverer and FluoroMatch.
- A semi-quantitative NTA approach was proposed using a global calibration curve to estimate total PFAS (concentrations).
- Non-traditional monitored PFAS were identified in surface and tap water from South Florida.
- CD and FluoroMatch showed to be complementary data processing methods for PFAS NTA.

GRAPHICAL ABSTRACT

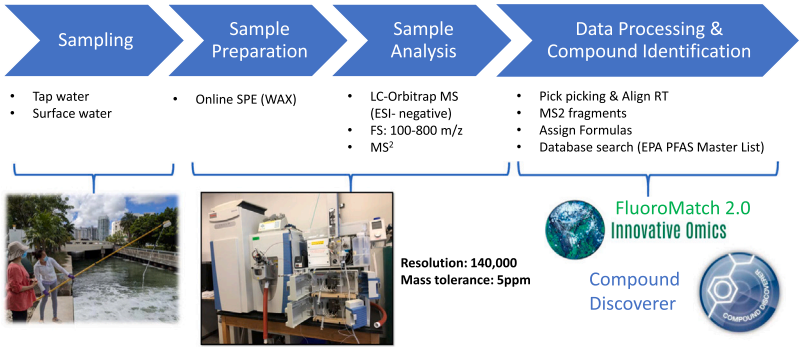

ARTICLE INFO

Editor: Lee Blaney

Keywords:
QNTA
Online SPE-LC-HRMS
Surface water
Tap water
Biscayne Bay

ABSTRACT

Per- and polyfluoroalkyl substances (PFAS) are a group of anthropogenic pollutants that are found ubiquitously in surface and drinking water supplies. Due to their persistent nature, bioaccumulative potential, and significant adverse health effects associated with low concentrations, they pose a concern for human and environmental exposure. With the advances in high-resolution mass spectrometry (HRMS) methods, there has been an increasing number of non-targeted analysis (NTA) approaches that allow for a more comprehensive characterization of total PFAS present in environmental samples. In this study, we have developed and compared NTA workflows based on an online solid phase extraction- liquid chromatography high resolution mass spectrometry (online SPE-LC-HRMS) method followed by data processing using Compound Discoverer and FluoroMatch for the screening of PFAS in drinking waters from populated counties in South Florida, as well as in surface waters from Biscayne Bay, Key west, and Everglades canals. Tap water showed the highest number of PFAS features, indicating a poor removal of these chemicals by water treatment or perhaps the breakdown of PFAS precursors. The high number of PFAS features identified only by CD and FluoroMatch emphasizes the complementary aspects of these data processing methods. A Semi-quantitation method for NTA (qNTA) was proposed using a global calibration curve based on existing native standards and internal standards, in which concentration estimates

* Corresponding author at: Department of Chemistry and Biochemistry, Florida International University, 11200 SW 8th Street, Modesto A. Maidique Campus, Miami, FL 33199, USA.

https://doi.org/10.1016/j.jhazmat.2023.131224
Received 6 January 2023; Received in revised form 25 February 2023; Accepted 14 March 2023
Available online 16 March 2023

were determined by a regression-based model and internal standard (IS) response factors. NTA play a crucial role in the identification and prioritization of non-traditionally monitored PFAS, needed for the understanding of the toxicological and environmental impact, which are largely underestimated due to the lack of such information for many PFAS.

1. Introduction

Per- and polyfluoroalkyl substances (PFAS) are a group of persistent contaminants that are found in aquatic environments ubiquitously worldwide [1,10]. PFAS molecules usually consist of C-F bonds which make them thermally and chemically stable [3]. Combined with their amphiphilic chemical properties, they are synthesized and valued in the production of a vast variety of commercial and consumer products, such as textiles, water/grease repellent, firefighting foam, paints, and non-stick coating [2]. However, recent in vivo and in vitro studies have shown that exposure to PFAS is associated with reproductive, developmental, hepatic, immunosuppressive, and endocrine disruptive toxicity [11]. In addition, PFAS are known to bioaccumulate through the food chain [34].

Though the production of perfluorooctanoic acid (PFOA) and perfluorooctane sulfonic acid (PFOS) has been banned in the U.S. due to health concerns, alternative PFAS molecules are brought into the market as replacements [8], which the impact on human health and the environment is still unclear. A few studies have reported that the emerging PFAS substitutes have shown similar toxicity and bioaccumulation compared to the banned legacy PFAS [18,29]. For example, PFBA showed higher accumulation in the lung and kidney than PFOS, whereas PFHxA showed preferred accumulation in human liver and brain tissue [29]. Toxicological studies have reported that exposure to PFAS substitutes such as perfluorobutanoic acid (PFBA), perfluorobutane sulfonic acid (PFBS), and perfluorohexanoic acid (PFHxA) induce hepatic, thyroid, and renal toxicity, as well as developmental delays ([5,18]. In addition to the continuous production of these emerging PFAS substitutes, the highly persistent legacy PFAS such as PFOA and PFOS are still found to be present in the environment worldwide, along with their degradation and transformation products [14]. As a result, the PFAS species in the environment are extremely diverse, with potentially over 10,000 compounds in existence that are covered in databases up to this date [31]. Current targeted analytical methods based on liquid chromatography (LC) - mass spectrometry (MS) applied to environmental water studies are able to detect up to 40–100 PFAS species (USEPA, 2021). Although targeted methods can achieve high sensitivity and accuracy, the number of PFAS molecules detected and quantified is restricted since it requires certified standards, many of which are not available at present for most PFAS. Thus, the environmental and public health risk associated with the "undetected" PFAS chemical space remains unknown.

There has been an increasing number of non-targeted analysis (NTA) approaches based on high-resolution mass spectrometry (HRMS) that allow for more comprehensive detection of total PFAS potentially present in environmental samples without the need for certified standards ([16,24]; [33]). The NTA workflow typically starts with obtaining HRMS full scan spectra and MS^2 spectra of a sample with no prior information needed, followed by data processing that involves obtaining quality features from large quantities of background features, as well as PFAS structural annotation using NTA software(s) based on different algorithms [15]. Since there is no established workflow or criteria for PFAS NTA screening, variability and uncertainty exist when it comes to differences in instrumentation, analytical method, NTA software used, and data processing criteria [14]. In addition, there is a need for harmonized approaches for quality assurance and quality control (QA/QC) among NTA analysis, including NTA for PFAS.

Previously, we developed a targeted analysis based on LC/MS and analyzed 30 PFAS in drinking and surface water from Florida [19]. A full assessment of both targeted and non-targeted approaches will be complementing the coverage of PFAS species identified in environmental samples, which plays a crucial role in further understanding their toxicological and environmental impacts. Therefore, in this study, we have developed a workflow for PFAS NTA screening based on an online solid phase extraction (SPE) coupled to a LC-HRMS method using a Q-Exactive Orbitrap system for the screening of PFAS species in drinking water from populated counties in South Florida, as well as in surface water from Biscayne Bay, Key West, and Everglades canals. Post-processing data reduction was conducted using the small molecules identification software Compound Discoverer 3.3 and FluoroMatch 2.0, a software specific for PFAS NTA, with the goal to compare the variability in processing NTA data for PFAS analysis in water samples. In addition, we propose a semi-quantitative NTA (qNTA) method to provisionally estimate total concentrations from PFAS identified without commercial standards. The method performance was assessed with spiked samples of 30 native standards (NS) and corresponding 19 isotope-labeled standards (IS). The semi-quantitative method was tentatively applied to the NTA results from the environmental water samples and concentrations were compared to the results from targeted analysis.

2. Materials and methods

2.1. Preparation of PFAS standards

A 30 native PFAS solution and 19 isotopically labeled PFAS mix were purchased from Wellington Laboratories Inc. (Guelph, Ontario, Canada) as native standards (NS) and internal standards (IS), respectively. Both stock solutions (1 mg/L in methanol) were further diluted to 10 μg/L in LC-MS grade water and stored at 4 °C for sample spiking. The list of PFAS in the standard solutions and labeled internal standards (IS) is presented in Table S1. Each water sample (QC samples were made with LC/MS water and environmental samples were used as collected) was spiked with 105 μL of 10 μg/L of labeled 19 PFAS IS mix to a final volume of 10.5 mL of water (making a resulting 100 ppt final IS concentration). Artificial seawater (3.5% w/v) was prepared using commercially available Instant Ocean sea salt according to the manufacture protocol (5.4 g sea salt powder in 150 mL LC-MS water).

2.2. Environmental samples

Water samples were collected in 500 mL pre-cleaned high-density polyethylene (HDPE) bottles with a swing arm sampler (Wooster, OH, USA), transported in a cooler with ice to the lab, and stored refrigerated at 4 °C until analysis. The HDPE bottles were rinsed with hexane, methylene chloride, methanol, and ultrapure water three times each, and air dried before collection to avoid potential PFAS contamination. Selected samples were from surface water samples of adjacent canals and water bodies of Biscayne Bay (N = 5), Key West (N = 3), and Everglades area (N = 3), as well as tap water samples (N = 6) from populated areas from South Florida (Pembrooke Pines, North Miami, Grapeland Heights, Fort Lauderdale, Miami Beach, and Davie). Details about the sampling sites and the concentration of 30 PFAS congeners that have been previously reported in our studies using a targeted LC-MS method are summarized in Table S2.

2.3. QA/QC

The Q-Exactive Orbitrap (Thermo Scientific) was calibrated in

positive and negative mode with mass tolerance < 5 ppm with Pierce LTQ ESI ion calibration solutions (Thermo Scientific). Quality control (QC) samples consisted of LC-MS grade water spiked with NS at final concentration of 50 and 100 ng/L and IS at final concentration of 100 ng/L to a final volume of 10.5 mL. QC samples were analyzed at the beginning of the sequence and every five environmental samples to ensure the instrument's performance. Blank samples (LC/MS grade water) were analyzed at the beginning and between every environmental sample; blanks and QC samples passed through the same sample preparation and data analysis process as the environmental samples. The chromograms of PFAS QC samples (native standards) showing the peak separation and intensity obtained by online SPE-LC-HRMS extracted by X-Calibur software through exact mass search is presented in Fig. S1. Detection limits were established as the lowest concentration where peak intensity was at least three times higher than that of a blank sample for each congener (inspected using targeted ion extraction). Matrix effects were evaluated with the artificial seawater samples and LC-MS water samples spiked with NS at the concentration of 0, 10, 50, 100, 500 ng/L. The confusion matrix was applied to evaluate the performance of the NTA method in terms of precision, accuracy, sensitivity, and specificity [12].

2.4. LC-MS/MS data acquisition

Data acquisition is based on an online SPE- liquid chromatography (LC)- HRMS method using a Q-Exactive Orbitrap system equipped with heated electrospray ionization (HESI) interface. Hypersil GOLD PFP HPLC Column (100 mm × 2.1 mm, 3 μm) was used for chromatogram separation. Waters Oasis WAX Online Column (20 mm × 2.1 mm, 30 μm) was used as the online SPE column. The mobile phase gradient program for the online SPE and analytical pumps are presented in table S3. The online procedure consists of a divert valve on the MS programmed by the data system, in which in the load position, 10 mL of sample were injected into a 10-mL loop and then loaded onto a SPE column by pump 2 (table S3), in this stage PFAS were retained in the WAX SPE column and the matrix that is not retained during the extraction process was directed to waste while simultaneously pump 1 equilibrates the analytical column in the starting gradient conditions. After 5 min, when the valve was switched to inject position, the solvent flow through the WAX SPE column was reversed, and PFAS were then backflushed onto a Hypersil Gold PFP column for separation and quantitation by HESI-MS/MS. After 19 min, the switching valve was returned to the loading position to allow the extraction column to be re-equilibrated with water. All samples, including blanks, calibration solutions, QA/QC and environmental samples were processed through the online SPE method. Water samples were run in full scan negative mode with a scan range from 100.0 to 800.0 m/z at a resolution of 140,000, followed by data-dependent MS/MS with a normalized collision energy of 30 and at a resolution of 35,000. Detailed MS parameters can be found in table S4.

2.5. Data post-processing

Two non-targeted workflows were established and optimized using Compound Discoverer (CD) 3.3 and FluoroMatch 2.0 from sample collection to data processing as shown in Fig. S2. Samples were post-processed with both software to screen for potential PFAS.

2.5.1. Compound discoverer 3.3

The data processing and annotation are based on the CD workflow "Environmental w Stats Unknown ID w Online and Local Database Searches" embedded in the software (Fig. S3). The databases searched included Chemspider, MzCloud, MzVault and the PFAS Master List in the U.S. EPA DSSTox. Peak picking and detection compounds nodules include a mass tolerance of 5 ppm and minimum peak intensity of 50,000. Elemental composition for molecular formula prediction was performed with maximum element counts of C90, H190, Br3, Cl4, F40, N10, O18, Na2, P3, and S5; considering a maximum atomic ratio of hydrogen to carbon (H:C) of 3.5. Pattern and fragment matching was performed at an intensity tolerance of 30%, an intensity threshold of 0.1%, a minimum spectral fit of 30%, and a minimum pattern coverage of 80%. The mass tolerance was set for < 5 ppm with a signal to noise ratio (S/N) of 3; blank subtraction was automatically performed by the software's algorithm using a blank sample. The samples from the same source (Biscayne Bay, Key West, Everglades, and tap water) were processed together in one batch, as well as Blanks and QC samples. The list of detected PFAS features generated by CD was further reduced by additional filtering criteria to improve confidence level, whereas only features meeting the criteria below were kept for further analysis: 1) mass defect ≥ 0.75 or ≤ 0.1, [26]; 2) Molecular Formula is proposed in the data file; 3) Mass list match was found in the EPA Master list [31]; 4) MS2 were found for preferred ion in Data Dependent Analysis (DDA); 5) class scoring > 6.25 for common fragments match (CF_3-, C_2F_5O-, etc.); and 6) the feature was found ≥ 2 samples from the same area. A feature is defined as a detected m/z, its retention time, and its intensity [28]. The final list of features detected in each location and type of water can be found in Table S5.

2.5.2. FluoroMatch 2.0

Data were processed on FluoroMatch software version 2.0 using the default setting parameters. Similar strategies were employed as in CD 3.3, in which the samples from the same source (Biscayne Bay, Key West, Everglades, and tap water) were processed in one batch. In the data output file, data were further reduced through manual curation based on the following criteria: 1) Exact Mass and MS2 Match in class-based standards and in-silico library; 2) Chemical Formula is proposed; 3) Score annotation in A (confident identification) [17]; and 4) Score annotation in B (highly likely PFAS identification). The final list of features detected from different sources by FluoroMatch can be found in Table S6.

2.6. Compound classification

The annotated PFAS were classified into several categories using 'PFAS-Map' which is a database framework tool that can automatically classify PFAS based on their SMILE structures. The structure classification is based on current PFAS classification criteria illustrated in [30]. The categories are classified as PFAS derivatives, PFAA, Perfluoro PFAA precursors, Non-PFAA perfluoroalkyls, FASA based PFAA precursors, Non-PFAA perfluoroalkyls, Fluorotelomer-based PFAA precursors, Silicon PFAS, side-chain Fluorinated aromatic PFAS, and other aliphatic PFAS.

2.7. Semi-quantification

The 30 native PFAS standards mix was used to prepare a five-point calibration curve at concentrations of 0, 10, 50, 100, and 500 ng/L. The labeled 19 PFAS IS mix was spiked to the standard calibration samples as well as water samples at a concentration of 100 ng/L for standardization, accounting for variabilities in sample preparation and LC-HRMS measurements. The average response (peak area) from all labeled 19 IS was used to normalize the average response of all 30 PFAS NS. A global calibration curve, which is an averaged curve made with all 30 PFAS and 19 labeled IS available in the lab, was plotted using a quadratic regression fit curve of the concentration (X) versus the response factor between the average response of NS and IS (peak area of the native standard/peak area of the internal standard). Thus, at each concentration level, the peak areas obtained for all PFAS were averaged and normalized (divided) by the average peak area of all labeled IS added. The total PFAS concentration in each sample was estimated based on the sum of peak area and response factor using this global calibration curve.

3. Results and discussion

3.1. QA/QC

QC samples at concentrations of 50 ng/L and 100 ng/L were run in the same condition as the environmental samples. The peak integration of 30 NS was processed with Xcalibur software and based on exact mass search. All 30 NS were able to be separated and detected chromatographically by their exact mass, as shown in Fig. S1. The instrument detection limits determined was 10 ng/L for all 30 NS prepared in LC-MS water, in which the peak intensity was in fact at least 10 times higher than blank samples and with S/N higher than 100. When the standards were prepared in artificial seawater (3.5% w/v), the instrument was still capable of detecting 10 ng/L for the majority of the compounds (S/N > 100), except for PFPeA, PFDoA, PFTrDA, 8–2 FTS and N-EtFOSAA that had detection limits of 50 ng/L. These results suggest that the Orbitrap MS could detect lower detection limit than 10 ng/L for some compounds, nevertheless the presence of background PFAS levels would become more critical at lower levels. The QC samples were analyzed through the NTA workflow by CD and FluoroMatch. The detected and identified features generated directly from both workflows manually curated followed the same criteria as for the environmental samples, which aimed at removing noise and falsely identified (false positive) compounds. For CD, the number of features was reduced from 2036 to 55 after applying filtering criteria, in which all 30 PFAS were correctly identified. True Positives (TPs) are the PFAS NS correctly identified, which in this case TPs= 30. False Positives (FPs) are the compounds incorrectly identified as true positives, in which FPs= 25. True negatives (TNs) are the PFAS correctly identified as not in the samples, TNs= 1981. False negatives (FNs) are the NS incorrectly identified, in this case FNs= 0. The confusion matrix is used to evaluate the performance of the NTA method as presented in Table 1 [12]. The true positive rate (TPR) is the proportion of the samples that were correctly reported as present relative to all compounds truly present in the sample, which represents the sensitivity of the method. In this case, all the 30 PFAS in the QC samples are correctly identified with TPR of 1. True negative rate (TNR) is the proportion of the compounds correctly reported as absent relative to all compounds that are truly absent in the sample, which represents the specificity or selectivity. The optimized NTA workflow with additional manual data post-processing was able to largely reduce falsely identified compounds with TNR of 0.98. The precision (0.55) is evaluated as the proportion of correctly identified compounds relative to all compounds reported present in the sample. The accuracy (0.99) is evaluated based on the proportion of compound correctly identified as present or absent relative to all reported compounds. For FluoroMatch, the number of features was reduced from 8226 to 27 after applying filtering criteria, in which 14 PFAS were correctly identified. According to performance matric, TP is 14, FP is 13, FN is 16, TN is 8212. Overall, both methods showed a very good accuracy (0.99–1) and specificity (0.99–1), although precision (0.52–0.55) could be improved by reducing further the number of false positives. This is one of the major obstacles in NTA, as further processing to reduce FP could impact the correct identifications (TP). CD showed higher sensitivity (1.0) than FluoroMatch (0.47), since it was able to identify all spiked PFAS NS.

Matrix effects (ME) were assessed by comparing the slope of calibration curve for standard solutions (NS in LC-MS water) with that of matrix matched standard solutions (NS in artificial seawater) using the formula ME (%) = (slope of the matrix-matched/slope in solvent) * 100%. The slope for matrix matched standard solution (slope=0.0174) was higher than that of standard solution in water (slope=0.0108) as seen in Fig. S4 which leads to a ME of 161% suggesting ion-enhancement in water samples with higher salinity [13].

3.2. Screening of PFAS in water samples from South Florida using Compound discoverer 3.3 and FluoroMatch

Based on the criteria outlined in Section 2.5, 255 features in total were filtered out by CD in the water samples from different sources, annotated with compound name, chemical formula, *m/z*, RT, class score, MS^2 and match in the EPA PFAS master list. The processed data file is presented in supplemental table S5. In Biscayne Bay samples, 29 tentatively identified PFAS were filtered out from 689 features (reported directly from the software). 7-(Heptafluoropropyl)− 4,9-dimethoxy-5 H-furo[3,2-*g*][1] benzopyran-5-one ($C_{16}H_9F_7O_5$), 1,1,2,2,3,3,5,5,6,6,6-undecafluoro-4,4-bis(trifluoromethyl)hexane-1-sulfonic acid ($C_8HF_{17}O_3S$), which is a bis isomer form of PFOS, and N-Carboxymethyl-N,N-dimethyl-2-(per fluoroethyl)− 2-fluoroethan-1-aminium ($C_8H_{12}F_6NO_2$) were found to be the most prevalent PFAS (highest peak intensity) in Biscayne Bay water samples. In tap water samples, 151 features were filtered out of 2216 features, whereas perfluoro-2-(trifluoromethyl)propanesulfonic acid ($C_4HF_9O_3S$), annotated as a branched isomer from PFBS (however this feature is not chromatographically distinguished from linear PFBS in the reference standard), 2,2,3,4,4,5,5,5-octafluoro-3-(trifluoromethyl)pentanoic acid ($C_6HF_{11}O_2$), annotated as a branched isomer from PFHxA (having coeluted retention time with the linear PFHxA in the reference standard), 1-chloro-2,2,3,3-tetrafluorocyclobutane ($C_4H_3ClF_4$) and perfluoro-p-ethylcyclohexylsulfonic acid ($C_8HF_{15}O_3S$) were the most prevalent species. In samples from Everglades adjacent canals, 75 were filtered out 1155 features; the prevalent PFAS included 6:2 fluorinated telomer sulfonate ($C_8H_5F_{13}O_3S$), 1-chloro-2,2,3,3-tetrafluorocyclobutane ($C_4H_3ClF_4$), followed by PFOS, PFBS, PFHxS. In Key West samples, 5 were filtered out of 196 features; the compounds 1,1,1,2,2,3,3-Heptafluoro-3-(2,2,2-trifluoroethoxy)propane ($C_5H_2F_{10}O$) and 4-(1,1,1,2,3,3,3-Heptafluoropropan-2-ylsulfanyl)− 2,6-dimethylaniline ($C_{11}H_{10}F_7NS$) were the prevalent species.

The Venn diagram in Fig. 1 shows the features that are unique or overlapping from different water sources. Tap water has the most detected features and unique features. This can be attributed to higher PFAS concentrations being prevalent in highly urbanized areas and the ineffective removal of these recalcitrant compounds or perhaps the breakdown of PFAS precursors by drinking water treatment plants [19,20,7]. Tap water also has the largest overlap (N = 23) with Everglades samples. This large overlap of features between tap water and water from the Everglades can be attributed to the fact that the major source of drinking water in South Florida is groundwater, coming especially from the Everglades aquifers. Everglades samples also shared 10 features with Biscayne Bay. These overlapping features can be a result of the adjacent canals near the Everglades flowing towards Biscayne Bay. The lower

Table 1
The performance metrics used to assess the NTA performance for Compound discoverer (CD) and FluoroMatch (FM).

True Positive (TP) TP= 30 (CD) TP= 14 (FM)	False Positive (FP) FP= 25 (CD) FP= 13 (FM)	$precision = \frac{TP}{TP+FP}$ Precision= 0.55 (CD) Precision= 0.52 (FM)
False Negative (FN) FN= 0 (CD) FN= 16 (FM)	True Negative (TN) TN= 1981 (CD) TN= 8212 (FM)	$Accuracy = \frac{TP+TN}{TP+FP+FN+TN}$ Accuracy= 0.99 (CD) Accuracy= 1.00 (FM)
True positive Rate (TPR) $TPR = \frac{TP}{TP+FN}$ Sensitivity= 1.00 (CD) Sensitivity= 0.47 (FM)	Ture Negative Rate (TNR) $TNR = \frac{TN}{TN+FP}$ Specificity= 0.99 (CD) Specificity= 1.00 (FM)	

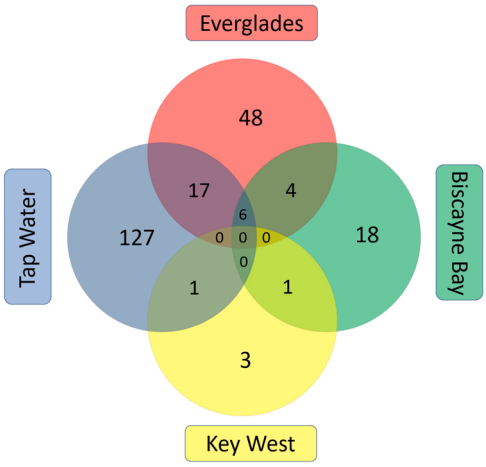

Fig. 1. Venn diagram of PFAS screened in water samples from different sources (Tap water, surface water from Biscayne Bay, Key West, and Everglades adjacent canal) using CD 3.3.

number of detected features in Biscayne Bay compared to the Everglades could be because as you go downstream, PFAS can be lost due to potential bioaccumulation into aquatic plants and organisms as well as susceptible to dilution effect ([22]; [32]). However, no feature was found in common among all four sources. The number of features in each different water source has been corroborated by previous studies that showed that the concentration of detected PFAS in tap water are higher than that of surface water, with surface water samples from Key West having very low concentrations of PFAS, leading to its low number of features detected by NTA [19,20].

The identified features from different water sources are visualized in the Kendrick mass defect (KMD) against the Nominal Kendrick Mass (NKM) plot, as shown in Fig. S5. The Kendrick mass (KM) of an observed mass (OM) is normalized by the ratio of nominal mass to the exact mass of the repeating unit of CF_2. The KMD is calculated as the difference between the NKM and exact KM. PFAS homologues series with only varying numbers of repeating units of CF_2 (m/z 49.9968) share the same KMD and thus align horizontally on the KMD plot. The KMD can be plotted based on different repeating units that are common to PFAS, such as CF_2O (m/z 65.9917) and C_2F_4O (m/z 115.9885) [9]. Due to fluorine atoms having a negative mass defect of $\Delta m/z = -0.0016$, PFAS have low and often increasingly negative mass defects as the number of fluorine atoms increases [21]. The plot presented here is based on the most common repeating unit of CF_2. Samples from different water sources are presented in Fig. S4 to visualize the difference between sample types. The tap water has the most detected features with the majority spanning the NKM range of 250–500 and mostly occupying the negative region of the KMD (−0.025 to −0.125). It was previously reported that the majority (> 90%) of PFAS from a curated PFAS list containing 3213 PFAS had a mass defect between − 0.25 and + 0.1 which was also observed in this study [4]. Water samples from Everglades adjacent canals show a similar pattern as tap water. In contrast, the samples from Biscayne Bay and Everglades are more evenly distributed on the positive and negative KMD, although there were very few features detected. The common overlapping area in which the majority of the features among all the sample types is observed is in the negative region of the KMD between NKM of 200–500.

A Van Krevelen diagram as shown in Fig. 2 is also presented to visualize the detected PFAS features of the water samples from different sources, in which the ratio of Fluorine and Carbon (F:C) is plotted against the ratio of oxygen to carbon (O:C) for each feature. Based on the degree of saturation and oxygen content, the features are localized in different regions on the Van Krevelen diagrams. As described in [27], for example, the compounds containing no oxygen (aromatic hydrocarbons) appear at the y-axis, and PFAS with high content of fluorine would appear in the upper region given the F/C ratio is relatively high, especially for a lot of the legacy PFAS where all the hydrogens on the carbon chain are substituted by fluorine. In our data, the clutter of more densely populated area appears to be in the region with F:C from 0.25 to 2.0, and O:C from 0 to 0.4, which suggest the majority of the PFAS has a low content of oxygen and are polyfluoroalkyl where H are only partially substituted by the fluorine in the carbon chain.

These water samples raw data were also post-processed using FluoroMatch, an open-source software tailored toward PFAS annotation [17]. This data post-processing yielded 129 features in total from the water samples from different sources, annotated with compound name, chemical formula, m/z, RT, matching fragments in-house library, and confidence score. The processed data file is presented in supplemental table S6. In Tap water samples, 55 PFAS were filtered out from 8227 features (reported directly from the output), whereas perfluorobutanesulfonic acid ($C_4HF_9O_3S$), perfluorooctanesulfonic acid ($C_8HF_{17}O_3S$), and PFOA ($C_8HF_{15}O_2$) were found to be the most prevalent PFAS (highest peak intensity). In Biscayne Bay (BB) samples, 32 features

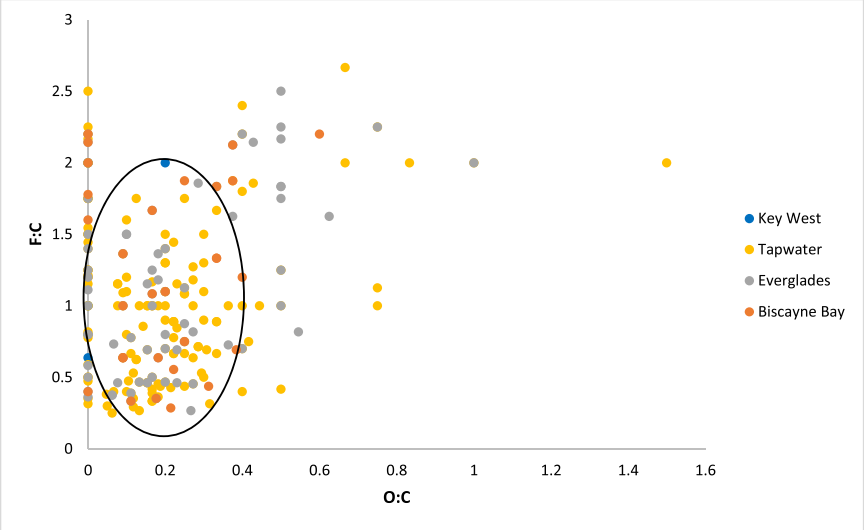

Fig. 2. Van Krevelen diagram of PFAS screened from different water sources using CD 3.3. The circle indicated the more densely populated area in the region with F:C from 0.25 to 2.0 and O:C from 0 to 0.4, which suggest the majority of the PFAS have a low content of oxygen and are polyfluoroalkyl.

were filtered out of 10416 features. 2-[chloro(difluoro)methoxy]− 1,1,2,2-tetrafluoroethanesulfonic acid ($C_3HClF_6O_4S$), perfluorobutane sulfonic acid ($C_4HF_9O_3S$), and PFPeS ($C_5HF_{11}O_3S$) were the most prevalent species in BB. In samples from Everglades adjacent canals, 22 were filtered out of 3249 features. The prevalent PFAS included 5-(1,1,2,2,3,3,4,4,4-nonafluorobutyl)− 1 H-pyrimidine-2,4-dione ($C_8H_3F_9N_2O_2$), chloro-perfluoropropane sulfonate ($C_3HClF_6O_3S$), and perfluoro-6-methylheptanecarboxylic acid ($C_9HF_{17}O_2$) in the Everglades canals. In Key West samples, 20 were filtered out of 3249 features, with 6:2 FTS ($C_8H_5F_{13}O_3S$) and 2,2,3,3,4,4,5,5,5-nonafluoropentanal (C_5HF_9O) being the prevalent species.

As shown in the Venn diagram in Fig. 3, the tap water has the most detected features followed by Biscayne Bay samples. Three features were in common by all four sources, which were tentatively identified as 1,1,2,3,3-pentafluoroprop-2-ene-1-sulfonic acid ($C_3HF_5O_3S$), which has not been previously identified in environmental samples and is not present in the PFAS Master List, PFBS ($C_4HF_9O_3S$, level 1a), and PFPeS ($C_5HF_{11}O_3S$, level 1a); whereas confidence level 1a represents PFAS confirmed by a reference standard [6].

The identified features from different sources are visualized in the plot of KMD against NKM as shown in Fig. S6. The tap water has the most detected features and is spread out on the nominal mass range between 200 and 500 and has both positive and negative KMD. However, water samples from Everglades adjacent canals clustered more on the negative region of KMD (−0.07 to 0.17). Features from different sources are also visualized as a Van Krevelen diagram in Fig. 4. The cluster of the more densely populated area appears to be in the region with F:C from 0.25 to 2.5, and O:C from 0 to 0.5, which suggest the majority of the PFAS compound has a slightly higher content of oxygen, and PFAS with the H completely or partially substituted by fluorine in the carbon chain both present in the features. Although the number of features detected by FluoroMatch is significantly less (79% less) than that of CD, the observed results in both Van Krevelen diagrams are very similar. One data point that falls out of the cluster is PFSA-pentafluorosulfide ($CHF_7O_3S_2$) found in tap water, which has an extremely high ratio of F due to the bonding to sulfur.

When comparing the results from Compound Discoverer and FluoroMatch, CD annotated 225 PFAS and FluoroMatch annotated 95 PFAS at a confidence level of 1a or 2a-2c (evidence of probable diagnostic fragmentation or homologue and in some cases with library match) according to Charbonnet et al. [6]. A total of 19 compounds were identified by chemical formula using both workflows, while 206 were unique to CD and 76 were unique to FluoroMatch, as shown in Fig. S7. The compounds found by both workflows include typical PFAS with level 1a confidence level identification: 6:2 FTS, PFHpA, PFHxS, PFHxA, PFBS, PFBA, [6] and some long chain nitrogen contained PFAS. These results reinforced the complementary characteristic of these data processing methods [25]. Even though the higher number of tentatively identified PFAS by CD would at first suggest that the latter might be better suited for the detection of a wider range of PFAS, it's possible that CD could have a higher rate of false positives when compared to FluoroMatch, which is an annotation tool that has been designed specifically for identification of PFAS.

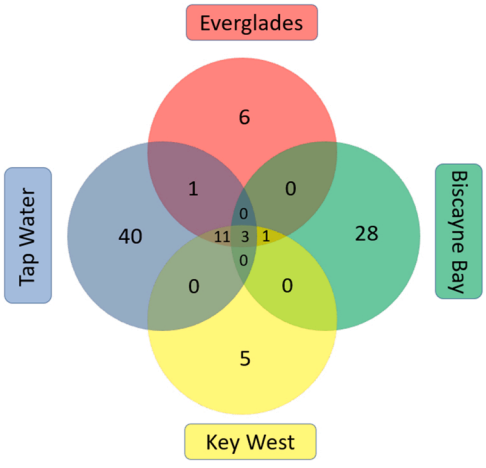

Fig. 3. Venn diagram of PFAS screened in water samples from different sources (Tap water, surface water from Biscayne Bay, Key West, and Everglades adjacent canal) using FluoroMatch.

The classification of annotated PFAS was explored using PFAS-MAP based on the SMILES structures. Based on the structure classification on PFAS-Map, 51% of the PFAS fell under the class of other aliphatic PFAS (perfluorocarbon units), 31% were classified as side-chain fluorinated aromatic PFAS (perfluorocarbon unit with aromatic bonds), 9% were attributed to perfluoroalkyl acids (PFAAs), mostly perfluoroalkyl carboxylic acids (PFCAs) and perfluoroalkane sulfonic acids (PFSAs), 4% of fluorotelomer-based PFAA precursors (n:2 fluorotelomer acrylates-FTACs, n:2 fluorotelomer methacrylates-FTMACs, n:2 fluorotelomer sulfonic acids-FTSAs, among others), 1% of non-PFAA perfluoroalkyl substances, and less than 1% (0.3–0.7% each) of PFAS halogen derivatives (containing chlorine or bromine), PFAS containing silicon, perfluoroalkyl PFAA precursors and other PFAS, demonstrating the wide range of classes identified by NTA.

3.3. PFAS Semi-quantitative assessments

qNTA was performed for PFAS tentatively identified with CD 3.3 using a global calibration curve created based on the available 30 PFAS NS. The global calibration curve for the NTA estimates is shown in Fig. S8. First, to estimate the accuracy of using the global calibration curve for concentration estimates, the concentration of a QC sample containing NS and IS spiked in LC-MS grade water (50 ng/L) was calculated based on the global calibration curve and compared to their added concentrations. The percentage error (PE) for each compound is presented in Table 2.

The PE of PFHpA, PFOA, PFNA, PFDA, FBSA, PFDS, and PFONS was overestimated by up to 50% of the actual concentration, and of PFPeA, PFUdA, FOSA, MeFOSAA was underestimated by up to 50%. The PE of PFHpS was overestimated by 51–100% of the actual concentration, whereas the compounds PFBA, PFDoA, PFTeDA, GenX, EtFOSAA, 4:2 FTS, 6:2 FTS, 8:2 FTS, NaDoNA, and PFOUds showed to be underestimated by 51–100%. The PE of FHxSA, PFBS, PFPeS, PFHxS, PFOS, PFNS was overestimated by over 100% of the actual concentration, and PFHxA and PFTrDA were underestimated by over 100%. Variations of systemic overestimation and underestimation are generally caused by using a global (averaged) calibration curve, especially with very diverse chemical structures of PFAS resulting in differences in ionization efficiency and chromatography [23]. With targeted analysis, these errors can be corrected when using isotopically labeled matching standards which leads to more accurate measurement. Although errors associated with individual PFAS measurements can be extremely high as seen in Table 2, when the total concentration of 30 PFAS was calculated, the result only presented 0.4% error when compared to the actual concentration (50 ng/L times 30 compounds) associated with the averaged response factors. This approach has limitations as the number of PFAS assessed might not be representative of the entire PFAS chemical space, in fact there is lack of commercially available standards for the majority of the PFAS, but seems to be a very promising simple and straightforward method in estimating "total" PFAS concentrations. The purpose of the qNTA shown here is to provide a provisional estimate of the total concentration of PFAS in a sample, which can provide complementary information for further studies on the toxicological and environmental impacts of PFAS.

The above qNTA method was applied to the data obtained in tap water samples from South Florida and environmental surface water samples collected from Biscayne Bay, Key West, and Everglades adjacent

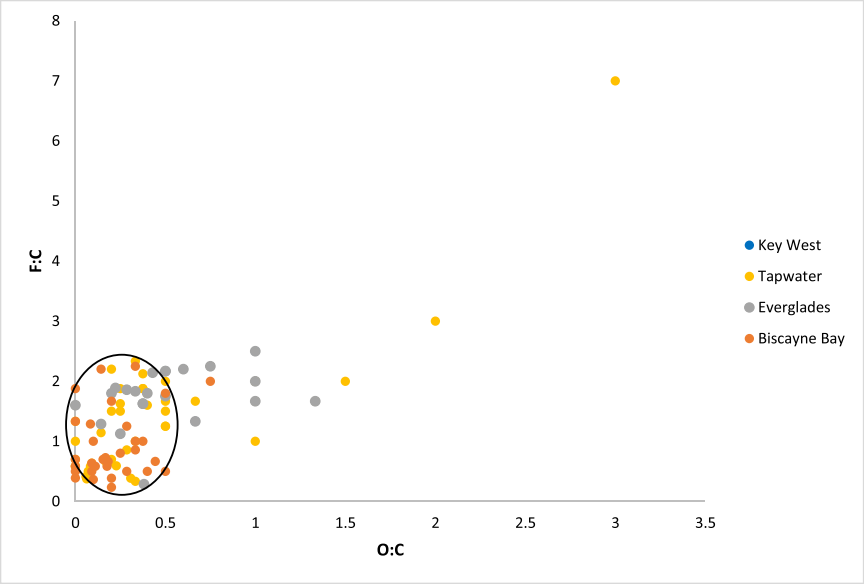

Fig. 4. Van Krevelen diagram of PFAS screened from different water sources using FluoroMatch. The circle indicated the more densely populated area in the region with F:C from 0.25 to 2.5 and O:C from 0 to 0.5, which suggest the majority of the PFAS compound has a slightly higher content of oxygen, and PFAS with the H completely or partially substituted by fluorine in the carbon chain both present in the features.

Table 2
The calculated concentration of 50 ng/L QC sample based on the global calibration curve. The percentage error (PE) for each NS is calculated compared to the actual concentration.

QC 50 ng/L	Calculated concentration in ng/L	Percentage error (%)
PFBA	0.51	-99
PFPeA	42.9	-14
PFHxA	-0.61	-101
PFHpA	59.1	18
PFOA	63.1	26
PFNA	66.7	33
PFDA	60.1	20
PFUdA	49.0	-1.92
PFDoA	19.3	-61
PFTrDA	-0.71	-101
PFTeDA	3.63	-93
FBSA	73.5	47
FHXSA	102	105
FOSA	29.7	-41
GenX	15.5	-69
MeFOSAA	27.6	-46
Et-FOSAA	23.1	-54
PFBS	163	226
PFPeS	121	143
PFHxS	120	140
PFHpS	90.6	81
PFOS	109	119
PFNS	105	111
PFDS	64.4	29
4:2 FTS	15.8	-68
6:2 FTS	16.7	-67
8:2 FTS	21.6	-57
NaDoNA	2.24	-96
PFONS	72.9	46
PFOUds	24.6	-51
Total	1563	0.4

canals. The total concentrations of all the PFAS tentatively identified in the sample were calculated based on the global calibration curve, which was compared to the total concentration of 30 PFAS from targeted analysis for each sample, as shown in Fig. 5.

The results from qNTA and targeted analysis are in the same order of magnitude for most samples from tap water, Biscayne Bay, and Key west samples, with the difference within the range of 9–116%. In general, the total PFAS concentration obtained from qNTA was lower than that calculated by targeted analysis, which represents only the sum of 30 PFAS. Even though it might be expected higher levels measured by qNTA since NTA incorporates much more species that were not quantifiable by quantitative targeted analysis (qTarget), conservative approaches to reduce false positives together with higher detection limits on the HRMS method could potentially explain the opposite outcome. Therefore, what could have contributed to the errors in the qNTA estimates is that many PFAS that were able to be detected in targeted analysis may not be detected in NTA due to their low concentrations in the environmental samples (detection limits of the targeted analysis were as low as 0.01–0.35 ng/L, whereas for NTA it was 10–50 ng/L). It has to be taken also into consideration the limitations of this approach which introduce errors (in some cases higher than 100%) coming from using the global calibration curve, therefore contributing to one to two orders of magnitude higher or lower than the actual value. In this aspect, the NTA data would be complementing PFAS concentrations found by targeted analysis. It was surprising that in the samples from the Everglades adjacent canals, PFAS total concentration estimated by qNTA is 2–7-fold higher than what was previously reported by targeted analysis, which could suggest a more complex composition of PFAS in higher concentration, which was neglected by the targeted analysis. Further investigation should focus on the potential sources of PFAS that could have contributed to this substantially elevated PFAS concentration revealed by NTA in the Everglades area.

4. Conclusion

A NTA workflow for the screening of emerging PFAS was developed and optimized, which could be also potentially applied for elucidation of PFAS degradants and transformation products. The method performance of the optimized NTA workflow was assessed using a mixture of 30 PFAS native standards as QC samples and a comparison between the open-source software FluoroMatch and the proprietary software Compound Discover v3.3 was conducted. When the workflow was applied for the screening of PFAS species in environmental samples, a total of over 300 PFAS were tentatively identified from drinking waters from populated counties in South Florida, as well as in surface waters from Biscayne Bay, Key west, and Everglades canals.

Data post-processing using CD (a total of 225 feature detected)

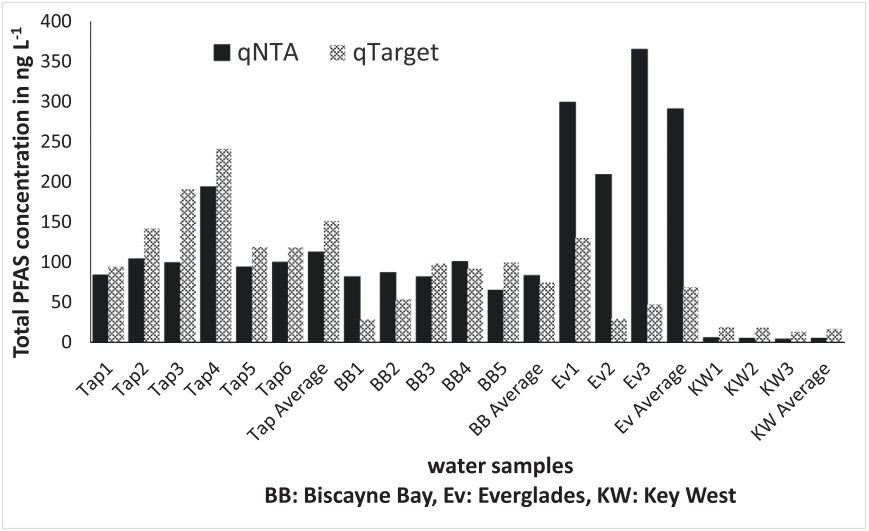

Fig. 5. Estimated total PFAS concentrations of water samples using a global calibration of 30 NS (qNTA) and concentrations of the samples using targeted analysis developed previously in Li et.al. 2022a,b.

yielded a greater number of PFAS species than FM (95 features), which could be an indication that CD may be better suited for the detection of a wider range of PFAS. Nevertheless, the high number of features uniquely identified only by CD (206) and FluoroMatch (76) emphasizes the complementary aspects of these data processing methods. The results showed tap water containing the greatest number of PFAS species (CD=151; and FM= 55), followed by Everglades (CD=75; FM=22) Biscayne Bay (CD=29; FM=32), and Key West (CD=5; FM=20), which could be potentially attributed to higher matrix effects caused by higher salinity content on the samples, especially in Key West. The higher overlapping of PFAS features between tap water and the Everglades is possibly due to drinking water in South Florida being supplied after treatment by groundwater sources including the Biscayne and Everglades aquifers.

A semi-quantitation method for NTA (qNTA) utilizing a “naïve” averaged global calibration curve on available native and labeled internal standards was explored and applied to environmental samples to estimate the "total” PFAS concentration. While a high error was observed when assessing individual PFAS (expected due to distinct ionization efficiencies between the compounds), it was less pronounced when considering the sum of PFAS (0.4% error), suggesting that this approach could provide an estimative of the total PFAS concentration, with limitations.

The concentration obtained from qNTA aggregates the ones previously measured by targeted analysis, which emphasize the importance of NTA in the detection and identification of a broader group of PFAS chemicals, including species not typically monitored by traditionally targeted analysis or that reference standards are not available. In special, it was found that total PFAS concentration estimated from qNTA in Everglades adjacent canals is 2–7-fold higher than from the previously reported targeted analysis, suggesting potential contamination sources coming from the Everglades area that needs to be further explored. Overall, NTA can provide complementary information on PFAS species in the environmental samples, which is needed to better evaluate their toxicological and potential impacts.

CRediT authorship contribution statement

Xuerong Li: Investigation, Methodology, Validation, Data curation, Visualization, Formal analysis, Writing – original draft, Writing – Draft reviewing. **Danni Cui:** Investigation, Validation, Data curation. **Brian Ng:** Methodology, Visualization, Writing – review & editing. **Olutobi Daniel Ogunbiyi:** Formal analysis, Data curation, Visualization. **Maria Guerra De Navarro:** Formal analysis, Data curation, Visualization, Review. **Piero Gardinali:** Resources, Writing – review & editing. **Natalia Quinete:** Conceptualization, Methodology, Validation, Data curation, Visualization, Formal analysis, Writing – review & editing, Project administration, Supervision, Resources, Writing – original draft, Writing – review & editing, Project administration, Supervision.

Declaration of Competing Interest

The authors declare that they have no known competing financial interests or personal relationships that could have appeared to influence the work reported in this paper.

Data Availability

Data will be made available on request.

Acknowledgements

We are thankful for financial support from FIU CREST Center for Aquatic Chemistry and Institute of Environment. Xuerong Li acknowledge the Dissertation Year Fellowship from Florida International University and Cristina Menendez Fellowship from FIU Institute of Environment’s Freshwater Resources Division. This material is based upon work supported by the National Science Foundation under Grant No. HRD-1547798 and Grant No. HRD-2111661. These NSF Grants were awarded to Florida International University as part of the Centers of Research Excellence in Science and Technology (CREST) Program. This is publication #1543 from the Institute of Environment , a Preeminent Program at Florida International University.

Environmental implications

A non-targeted analysis for the comprehensive identification of PFAS by Compound Discoverer and FluoroMatch based on online-SPE-LC-Orbitrap MS was developed, where non-traditionally monitored PFAS were tentatively identified in different water sources in South Florida. A semi-quantitation approach was proposed based on a global calibration curve to improve the understanding on total PFAS levels in environmental samples, which contributes to improve ecological and health risks assessments associated with PFAS exposure.

Appendix A. Supporting information

Supplementary data associated with this article can be found in the online version at doi:10.1016/j.jhazmat.2023.131224.

References

[1] Ahrens, L., 2011. Polyfluoroalkyl compounds in the aquatic environment: a review of their occurrence and fate. J Environ Monit 13 (1), 20–31. https://doi.org/10.1039/C0EM00373E.

[2] Buck, R.C., Korzeniowski, S.H., Laganis, E., Adamsky, F., 2021. Environmental policy & regulation identification and classification of commercially relevant per- and poly-fluoroalkyl substances (PFAS). Integr Environ Assess Manag 17 (5), 1045–1055. https://doi.org/10.1002/ieam.4450.

[3] R.C. Buck, P.M. Murphy, M. Pabon, Springe Berl Heidelb 2011 1 24 doi: 10.1007/978-3-642-21872-9_1.

[4] Bugsel, B., Zwiener, C., 2020. LC-MS screening of poly- and perfluoroalkyl substances in contaminated soil by Kendrick mass analysis. Anal Bioanal Chem 412 (20), 4797–4805. https://doi.org/10.1007/s00216-019-02358-0.

[5] Chang, S.-C., Das, K., Ehresman, D.J., Ellefson, M.E., Gorman, G.S., Hart, J.A., et al., 2008. Comparative pharmacokinetics of perfluorobutyrate in rats, mice, monkeys, and humans and relevance to human exposure via drinking water. Toxicol Sci 104 (1), 40–53. https://doi.org/10.1093/toxsci/kfn057.

[6] Charbonnet, J.A., McDonough, C.A., Xiao, F., Schwichtenberg, T., Cao, D., Kaserzon, S., et al., 2022. Communicating confidence of per- and polyfluoroalkyl substance identification via high-resolution mass spectrometry. Environ Sci Technol Lett 9 (6), 473–481. https://doi.org/10.1021/acs.estlett.2c00206.

[7] Cui, D., Li, X., Quinete, N., 2020. Occurrence, fate, sources and toxicity of PFAS: What we know so far in Florida and major gaps. TrAC Trends Anal Chem 130, 115976. https://doi.org/10.1016/J.TRAC.2020.115976.

[8] Dhore, R., Murthy, G.S., 2021. Per/polyfluoroalkyl substances production, applications and environmental impacts. Bioresour Technol 341, 125808. https://doi.org/10.1016/j.biortech.2021.125808.

[9] Dimzon, I.K., Trier, X., Frömel, T., Helmus, R., Knepper, T.P., de Voogt, P., 2016. High resolution mass spectrometry of polyfluorinated polyether-based formulation. J Am Soc Mass Spectrom 27 (2), 309–318. https://doi.org/10.1007/s13361-015-1269-9.

[10] Domingo, J.L., Nadal, M., 2019. Human exposure to per- and polyfluoroalkyl substances (PFAS) through drinking water: a review of the recent scientific literature. Environ Res 177, 108648. https://doi.org/10.1016/J.ENVRES.2019.108648.

[11] Fenton, S.E., Ducatman, A., Boobis, A., Dewitt, J.C., Lau, C., Ng, C., et al., 2021. Per-and polyfluoroalkyl substance toxicity and human health review: current state of knowledge and strategies for informing future research. Environ Toxicol Chem 40 (3), 606–630. https://doi.org/10.1002/etc.4890.

[12] C.M. Fisher, K.T. Peter, S.R. Newton, A.J. Schaub, J.R. Sobus, Approaches Assess Perform High-Resolut Mass Spectrom Non-Target Anal Methods 2022 doi: 10.1007/s00216-022-04203-3.

[13] Gosetti, F., Mazzucco, E., Zampieri, D., Gennaro, M.C., 2010. Signal suppression/enhancement in high-performance liquid chromatography tandem mass spectrometry. J Chromatogr A 1217 (25), 3929–3937. https://doi.org/10.1016/j.chroma.2009.11.060.

[14] Guelfo, J.L., Korzeniowski, S., Mills, M.A., Anderson, J., Anderson, R.H., Arblaster, J.A., et al., 2021. Environmental sources, chemistry, fate, and transport of per- and polyfluoroalkyl substances: state of the science, key knowledge gaps, and recommendations presented at the August 2019 SETAC focus topic meeting. Environ Toxicol Chem 40 (12), 3234–3260. https://doi.org/10.1002/etc.5182.

[15] Hollender, J., Schymanski, E.L., Singer, H.P., Ferguson, P.L., 2017. Nontarget Screening with High Resolution Mass Spectrometry in the Environment: Ready to Go. Environ Sci Technol 51 (20), 11505–11512. https://doi.org/10.1021/acs.est.7b02184.

[16] Jacob, P., Barzen-Hanson, K.A., Helbling, D.E., 2021. Target and nontarget analysis of per- and polyfluoralkyl substances in wastewater from electronics fabrication facilities. Environ Sci Technol 55 (4), 2346–2356. https://doi.org/10.1021/acs.est.0c06690.

[17] Koelmel, J. P., Stelben, P., Mcdonough, C. A., Dukes, D. A., Aristizabal-Henao, J. J., Nason, S. L., Li, Y., Sternberg, S., Lin, E., Beckmann, M., Williams, A. J., Draper, J., Finch, J. P., Munk, J. K., Deigl, C., Rennie, E. E., Bowden, J. A., & Pollitt, K. J. G. (n. d.). Fluoro Match 2.0-making automated and comprehensive non-targeted PFAS annotation a reality. https://doi.org/10.1007/s00216-021-03392-7/Published.

[18] Li, F., Duan, J., Tian, S., Ji, H., Zhu, Y., Wei, Z., et al., 2020. Short-chain per- and polyfluoroalkyl substances in aquatic systems: Occurrence, impacts and treatment. Chem Eng J 380, 122506. https://doi.org/10.1016/J.CEJ.2019.122506.

[19] Li, X., Fatowe, M., Cui, D., Quinete, N., 2022. Assessment of per- and polyfluoroalkyl substances in Biscayne Bay surface waters and tap waters from South Florida. Sci Total Environ *806*. https://doi.org/10.1016/j.scitotenv.2021.150393.

[20] Li, X., Fatowe, M., Lemos, L., Quinete, N., 2022. Spatial distribution of per- and polyfluoroalkyl substances (PFAS) in waters from Central and South Florida. Environ Sci Pollut Res. https://doi.org/10.1007/s11356-022-21589-w.

[21] Liu, Y., D'Agostino, L.A., Qu, G., Jiang, G., Martin, J.W., 2019. High-resolution mass spectrometry (HRMS) methods for nontarget discovery and characterization of poly- and per-fluoroalkyl substances (PFASs) in environmental and human samples. TrAC Trends Anal Chem 121, 115420. https://doi.org/10.1016/j.trac.2019.02.021.

[22] Martin, J.W., Mabury, S.A., Solomon, K.R., Muir, D.C.G., 2013. Progress toward understanding the bioaccumulation of perfluorinated alkyl acids. Environ Toxicol Chem 32 (11), 2421–2423. https://doi.org/10.1002/etc.2376.

[23] McCord, J., Newton, S., Strynar, M., 2018. Validation of quantitative measurements and semi-quantitative estimates of emerging perfluoroethercarboxylic acids (PFECAs) and hexfluoroprolyene oxide acids (HFPOAs. J Chromatogr A 1551, 52–58. https://doi.org/10.1016/J.CHROMA.2018.03.047.

[24] McCord, J., Strynar, M., 2019. Identification of per- and polyfluoroalkyl substances in the cape fear river by high resolution mass spectrometry and nontargeted screening. Environ Sci Technol 53 (9), 4717–4727. https://doi.org/10.1021/acs.est.8b06017.

[25] Nason, S.L., Koelmel, J., Zuverza-Mena, N., Stanley, C., Tamez, C., Bowden, J.A., et al., 2021. Software comparison for nontargeted analysis of PFAS in AFFF-contaminated soil. J Am Soc Mass Spectrom 32 (4), 840–846. https://doi.org/10.1021/jasms.0c00261.

[26] S.L. Nason, J. Koelmel, N. Zuverza-Mena, C. Stanley, C. Tamez, J.A. Bowden, K.J.G. Pollitt Softw Comp Nontargeted Anal PFAS AFFF-Contam Soil 2020 doi: 10.1021/jasms.0c00261.

[27] Ng, B., Quinete, N., Gardinali, P., 2022. Environmental chemistry differential organic contaminant ionization source detection and identification in environmental waters by nontargeted analysis. Environ Toxicol Chem 41 (5), 1154–1164. https://doi.org/10.1002/etc.5268.

[28] Pastore, C., Barca, E., del Moro, G., di Iaconi, C., Loos, M., Singer, H.P., et al., 2018. Comparison of different types of landfill leachate treatments by employment of nontarget screening to identify residual refractory organics and principal component analysis. Sci Total Environ 635, 984–994. https://doi.org/10.1016/j.scitotenv.2018.04.135.

[29] Pérez, F., Nadal, M., Navarro-Ortega, A., Fàbrega, F., Domingo, J.L., Barceló, D., et al., 2013. Accumulation of perfluoroalkyl substances in human tissues. Environ Int 59, 354–362. https://doi.org/10.1016/J.ENVINT.2013.06.004.

[30] Su, A., Rajan, K., 2021. A database framework for rapid screening of structure-function relationships in PFAS chemistry. Sci Data 8 (1), 14. https://doi.org/10.1038/s41597-021-00798-x.

[31] USEPA. (2020). PFAS Masterlist of PFAS Substances, United States Environmental 266 Protection Agency.

[32] Wang, Q., Tsui, M.M.P., Ruan, Y., Lin, H., Zhao, Z., Ku, J.P.H., et al., 2019. Occurrence and distribution of per- and polyfluoroalkyl substances (PFASs) in the seawater and sediment of the South China sea coastal region. Chemosphere 231, 468–477. https://doi.org/10.1016/J.CHEMOSPHERE.2019.05.162.

[33] Wang, Y.Q., Hu, L.X., Liu, T., Zhao, J.H., Yang, Y.Y., Liu, Y.S., et al., 2022. Per- and polyfluoralkyl substances (PFAS) in drinking water system: target and non-target screening and removal assessment. Environ Int 163, 107219. https://doi.org/10.1016/J.ENVINT.2022.107219.

[34] Xu, J., Guo, C.-S., Zhang, Y., Meng, W., 2014. Bioaccumulation and trophic transfer of perfluorinated compounds in a eutrophic freshwater food web. Environ Pollut 184, 254–261. https://doi.org/10.1016/j.envpol.2013.09.011.